Characterization and Activity of Ferric−Sulfide-Based Catalyst in Model Reactions of Direct Coal Liquefaction: Effect of Preparation Conditions

ARTICLE *in* INDUSTRIAL & ENGINEERING CHEMISTRY RESEARCH · FEBRUARY 1997

Impact Factor: 2.59 · DOI: 10.1021/ie960455q

Characterization and Activity of Ferric-Sulfide-Based Catalyst in Model Reactions of Direct Coal Liquefaction: Effect of Preparation Conditions

Ajay Chadha,[†] Charter D. Stinespring, Alfred H. Stiller, John W. Zondlo, and Dady B. Dadyburjor*

Department of Chemical Engineering, P.O. Box 6102, West Virginia University, Morgantown, West Virginia 26506-6102

We have studied the activity of various ferric-sulfide-based catalysts in model hydrogenation and cracking reactions under conditions typical of direct coal liquefaction (DCL). The catalysts used were mixtures of FeS_2 (pyrite, PY) and nonstoichiometric FeS_x (pyrrhotite, PH) obtained by high-temperature disproportionation of ferric sulfide in a nitrogen atmosphere or a hydrogen atmosphere. The structural changes in the catalyst were also examined, both before and after the model reactions. The cracking functionality of the catalysts was studied by using cumene, and the hydrocracking functionality was studied by using diphenylmethane. Phenanthrene was used as a model compound for hydrogenation and hydrogen shuttling. Phenanthrene hydrogenation was studied in the presence of H_2(g), and hydrogen shuttling was studied when a hydrogen donor (tetralin) was present in the absence of H_2(g). All the model reactions were performed under conditions typical of DCL: 400 °C and 1000 psig for 30 min. The surface and bulk of the catalysts were characterized by Auger electron spectroscopy, scanning electron microscopy, energy-dispersive X-ray spectroscopy, and atomic absorption spectroscopy. The performance of the catalysts was found to vary with the type of reaction, the initial ratio of FeS_x to FeS_2 (PH/PY) found in the catalyst, and the catalyst age. Catalysts freshly prepared in a nitrogen atmosphere were most active for model hydrogenation and hydrocracking runs. Catalysts freshly prepared in hydrogen were most active in shuttling. In all cases, catalytic cracking was negligible. Aging was found to reduce the activity of the catalyst. After the exposure of the catalyst to H_2(g) at 375 °C, the ratio PH/PY increased, but only limited changes in the PH/PY ratio were noted in a helium atmosphere. The surface uniformity of the catalyst was reduced after the catalyst reacted in H_2(g) or He(g). A simple model was developed to explain these changes in the surface and bulk of the catalysts. The model incorporates the hydrogenation of PY to PH and the removal of elemental S to form H_2S. The further interaction of H_2S with the catalyst surface makes it nonuniform, with S-deficient and S-rich sites. In the absence of hydrogen, surface reconstruction involves elemental S (from the disproportionation of the ferric sulfide) interacting with PH to form PH with a larger value of x, or PY in the limit.

Introduction

Direct coal liquefaction (DCL) refers to the formation of fuel-range products from coal, generally in the presence of a solvent and hydrogen, with or without the presence of a catalyst. Weak bonds in the coal are broken, probably by a thermolytic mechanism, at temperatures as low as 250 °C. The presence of a catalyst assists in the cleavage of these bonds, and the presence of hydrogen stabilizes the radicals (Vernon, 1980). In the presence of the catalyst, the solvent also assists in the cleavage of aryl−alkyl bonds (Malhotra and McMillen, 1993). Several mechanisms have been postulated to explain the role of the catalyst in hydrogen transfer and hydrogenolysis of moeties of coal; see, *e.g.*, Derbyshire (1989).

Recent emphasis has been placed on the development of low-cost "throw-away" iron-based catalysts for DCL. These catalysts are cheap and environmentally benign and provide the necessary activity without the need to undertake a costly catalyst recovery step. However, due to the complexity of the structure of coal, it is difficult to study catalyst activity and selectivity in actual DCL. These catalysts are also expected to change during DCL, with sulfide forms ranging from the pyrite (FeS_2, PY) to nonstoichiometric pyrrhotite (FeS_x, $x \approx 1$; PH). Further, a variety of coal products are obtained from DCL, and these are extremely difficult to characterize. Therefore, it is difficult to optimize conditions, to sort out desired processes, and to obtain meaningful information about catalyst activity and selectivity in DCL runs. One possible alternative is the use of simple compounds as reactants for model reactions of importance in DCL.

Model compounds have been used earlier to clarify different concepts of complex DCL reactions and DCL catalysis. Researchers have tried to identify the catalytically active chemical state of iron-based catalysts: PY, PH, the H_2S formed during the PY-to-PH conversion, or a combination of these components. Different model compounds have been used. The hydrogenolysis of benzothiophene was used by Guin *et al.* (1980) to study the hydrocracking activity of PY at DCL conditions. Kamiya *et al.* (1983) used the hydrogenation of phenanthrene and the cracking of *trans*-stilbene to study the effect of coal minerals in DCL. Ogawa *et al.* (1984), Hei *et al.* (1986), and Sweeny *et al.* (1987) used the hydrocracking reaction of diphenylmethane (DPM)

* To whom correspondence should be addressed. Telephone: (304) 293-2111 ext 411. Fax: (304) 293-4139. E-mail: dadyburjor@cemr.wvu.edu.

[†] Present address: United Catalysts Inc., P.O. Box 32370, Louisville, KY 40232.

S0888-5885(96)00455-1 CCC: $14.00

to study the H_2-H_2S-PH interaction. Montano *et al.* (1986) studied the hydrogenation of diphenyl ether in the presence of PH and H_2. Ogawa *et al.* (1984) indicated that PY is a more active promoter of coal liquefaction than is PH under H_2 and that PY formation from PH increases with increasing H_2S pressure. More recently, Farcasiu and Smith (1991) have studied the activity of catalysts in model compounds such as 4-(1-naphthylmethyl)bibenzyl, which contains polyfunctional moieties resembling coal molecules.

While model compounds have been widely used to understand the activity of iron-based DCL catalysts, most researchers have dealt with studying only limited functionalities of the catalyst. Further, a concurrent study of the changes in the catalyst during model coal liquefaction reactions is missing in most of the past research work. A comprehensive approach to study the overall activity and changes of iron-sulfide-based catalyst, in different model reactions, is needed to develop a better understanding of the catalyst.

We have tried to overcome some of the above-mentioned limitations by studying the activity of catalysts in different model reactions which are known to occur during coal liquefaction. Simultaneously, we have studied the changes in the catalyst bulk and the surface, before and after the model reactions. The catalysts used in the present work are all based on a ferric sulfide precursor, used extensively in our laboratory. Ferric sulfide is unstable even below room temperature and disproportionates into PY, PH, and elemental S as necessary.

$$\underset{\text{ferric sulfide}}{Fe_2S_3} \rightarrow \underset{\text{PY}}{\alpha FeS_2} + \underset{\text{PH}}{(2-\alpha)FeS_x} + (3 - 2\alpha + \alpha x - 2x)S \quad (1)$$

The relative amount of PH and PY, as well as the type of PH formed (*i.e.*, the value of *x*), depends on the time, temperature, pressure, and vapor-phase composition of disproportionation. In our laboratory, we have prepared these catalysts in a variety of ways, including hydrothermal (Stansberry *et al.*, 1993), *in-situ* disproportionation (Liu *et al.*, 1996), aerosol (Stiller *et al.*, 1995) and reverse-micelle (Chadha *et al.*, 1996) techniques.

The primary criterion for the selection of model compounds in our study is that the model compound reactions should mimic the actual chemistry taking place in DCL. The two foremost reactions where catalysts play an important role in the generation of reactive radicals are (a) hydrogenation, where there is a transfer of an H-atom to the *ipso* position of coal molecules, and (b) cracking, involving breakage of C−C bonds. Consistent with this, the reactions of our model compounds are hydrogenation and cracking reactions which are possible at DCL conditions. It is most significant that these model compounds do not show any activity at the DCL conditions in the absence of the catalysts. A detailed description of our model reactions, the experimental procedure, and techniques used in the analysis of these model reactions and catalysts are discussed in the next section.

Experimental Section

Model Reactions. Two modes of hydrogenation were considered: vapor-phase hydrogenation, using H_2(g), and liquid-phase shuttling, from solvent (tetralin). Two modes of cracking were considered: one without vapor-phase hydrogen and the other, hydrocracking, in the presence of H_2(g).

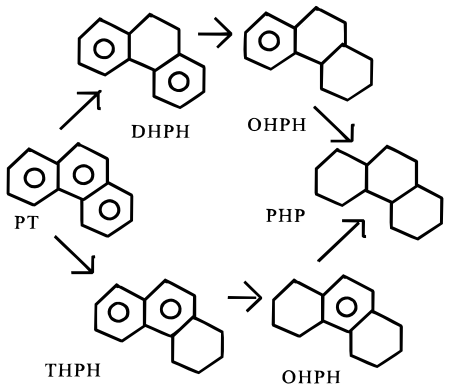

Figure 1. Products of phenanthrene hydrogenation (Whitehurst *et al.*, 1980). (PT = phenanthrene; DHPH = 9,10-dihydrophenanthrene; THPH = 1,2,3,4-tetrahydrophenanthrene; OHP = 1,2,3,4,5,6,7,8-octahydrophenanthrene; PHP = perhydrophenanthrene.)

Phenanthrene was used as the model compound to study the hydrogenation activity from the vapor phase. This compound was chosen because three-ring and higher structures are also found in the structure of coal. The products of the reaction are shown in Figure 1.

For the shuttling model run, tetralin was used as the hydrogen donor and phenanthrene as the acceptor. The products of the reaction are shown in Figure 2. These compounds were chosen to simulate hydrogen shuttling from a process solvent to the three- and four-membered aromatic ring compounds in coal. Tetralin, with four hydrogen atoms at the hydrogenated sites, is a good hydrogen donor and is often used in DCL studies.

The cracking activity was studied in a model reaction using cumene in the absence of hydrogen. Helium was used as the gas phase. The reaction can be written as

$$\underset{\text{cumene}}{C_6H_5-C_3H_7} \rightarrow \underset{\text{benzene}}{C_6H_6} + \underset{\text{propylene}}{C_3H_6} \quad (2a)$$

The cracking reaction is to simulate the breaking of aliphatic bridges in coal without hydrogen. Cumene was chosen because it requires acid sites of medium strength for cracking to occur (Liu and Dadyburjor, 1992).

Hydrocracking activity was studied using diphenylmethane (DPM) as a model compound. The reaction can be written as

$$\underset{\text{diphenylmethane}}{C_6H_5-CH_2-C_6H_5} + H_2 \rightarrow \underset{\text{benzene}}{C_6H_6} + \underset{\text{toluene}}{C_6H_5-CH_3} \quad (2b)$$

This reaction simulates the cracking of alkyl bridges which requires simultaneous hydrogenation (Lee and Montano, 1984).

As mentioned earlier, all these reactions were carried out initially in the absence of any catalyst and then with each of the catalysts described below. Additionally, runs were carried out in the presence of the catalyst but without the liquid-phase reactants; *i.e.*, the catalysts were heated in helium and in hydrogen under reaction conditions.

Catalysts. Two ferric-sulfide-based catalysts were used in the model reaction studies. The ferric sulfide was synthesized in a cold room starting from ferric chloride and sodium sulfide. The ferric sulfide was sealed in glass ampules and disproportionated (*via* eq

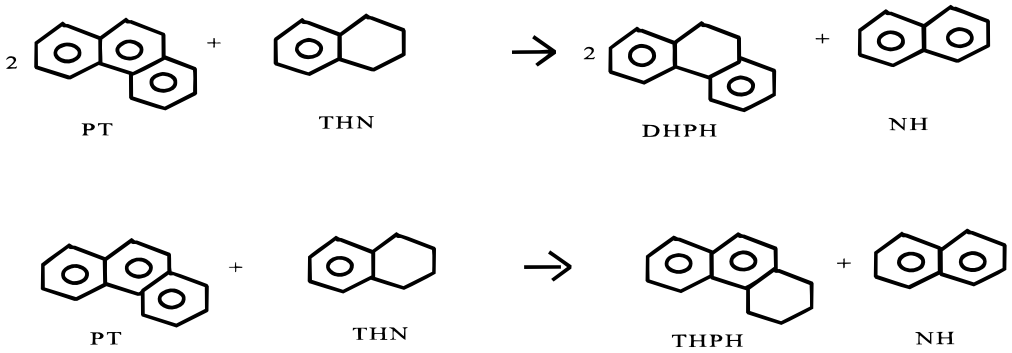

Figure 2. Phenanthrene hydrogenation from H-donor (tetralin). (PT = phenanthrene; DHPH = 9,10-dihydrophenanthrene; THPH = 1,2,3,4-tetrahydrophenanthrene; THN = 1,2,3,4-tetrahydrophenanthrene; THN = tetrahydronaphthalene; NH = naphthalene.)

1) in two ways. In one way, the ampule was placed in a bomb and heated to 200 °C in a nitrogen atmosphere. The presence of water outside the ampule, but in the bomb, maintained the integrity of the ampule. This was considered hydrothermal disproportionation in a nitrogen atmosphere. In the second procedure, the ampule was broken and placed upright in the bomb. The bomb was then flushed quickly several times with hydrogen, then sealed, and heated to 375 °C. This was considered hydrothermal disproportionation in a hydrogen atmosphere. These catalysts were used "fresh", *i.e.*, as prepared, and are termed NF and HF, respectively.

In addition, some of the runs were carried out with samples of similar catalysts that had been "aged" by being sealed in vials and stored in a cold room at 5 °C for $1^1/_2$ yr. These catalysts are termed NA and HA, respectively.

A few runs were carried out using a catalyst which was made in an aerosol reactor and similarly aged. This catalyst is termed EA. Detailed discussion on the synthesis of these catalysts may be found in Stansberry *et al.* (1993) and Stiller *et al.* (1995).

Chemicals and Gases for Model Reactions. The chemicals used in the model reactions, *viz.*, phenanthrene (98% purity), diphenylmethane (99% purity), cumene (98% purity), and tetralin (99% purity), were obtained from Aldrich Chemical Co. and were used as received. Hydrochloric acid (6 N) and nitric acid (8 N), used to wash the catalysts for the evaluation of the forms of Fe, and methylene chloride (99.9% purity), used to collect and dissolve the solid or liquid reaction products from the reactor, were also obtained from Aldrich Chemical Co. and again were used as received. Methanol (99%), obtained from Fisher Scientific, was used to wash the catalyst surface to remove elemental sulfur. High-grade helium with ultrahigh purity was used to pressurize the reactor in some model reactions. This gas was obtained from Matheson Gas Co. Regular-grade nitrogen (used to purge the glovebox), hydrogen (used in model reactions), and carbon dioxide (used to make dry ice) were obtained from West Virginia Welding Co.

Experimental Procedure. The model reactions were performed under the same conditions that direct coal liquefaction (DCL) runs are performed under in our laboratory. Reactions were carried out in the batch mode. The reactors were 17-cm^3 stainless-steel tubing-bomb reactors with Swagelok end caps. Welded to the center of the tube, and perpendicular to its axis, was a 0.25-in.-diameter stainless-steel tube connected to a needle valve, used for gas flow. For the case of hydrogen shuttling, 2 g apiece of phenanthrene and tetralin were loaded into the reactor; in all other cases, 4 g of the liquid feed was loaded into the reactor. For the catalytic runs, 0.5 g of the catalyst was placed in the reactor. The reactor end caps were then sealed. The appropriate gas, H_2 or He, was introduced through the needle valve to 1000 psig at room temperature. A set of two reactors was then agitated vertically at 400 rpm. A preheated sand bath was then raised until the reactors were fully immersed, and the reactor temperature was increased to 400 °C within 2 min. The total reaction time was 30 min. All runs were carried out in duplicate or greater, with reproducibility in conversion of approximately 0.1%.

The model reactions were also carried out in the absence of catalyst. These runs were expected to quantify the homogeneous reactions and also to determine any catalytic effect from the reactor surface.

Analysis of the Reaction Products. At the end of the reaction, both gaseous and liquid products were analyzed. The gaseous products were first vented into an evacuated flask of 250 mL. A 0.2-mL gas sample was collected from the flask and analyzed by means of a Shimadzu gas chromatograph (GC-8A) with a Hayesep D 100/120 Alltech packed column (20 ft × $^1/_8$ in. × 0.085 in.) and a thermal-conductivity detector (TCD). Hydrogen was used as the carrier gas. After the gaseous products were analyzed, the reactor was slowly filled with methylene chloride introduced through the needle valve. The needle valve was closed, and the reactor was placed on a shaker mechanism. This ensures proper dissolution of reaction products in methylene chloride. After shaking for 2−3 min, the reactor was opened from one end. The reaction products and the catalyst particles were removed, and the reactor was thoroughly cleaned with a wire brush. The reactor was then washed with methylene chloride, which was collected with the products. The catalyst particles were separated by vacuum filtration using a dry-ice cold trap and were separately analyzed. The liquid products were analyzed by an HP-5730A gas chromatograph with an OV-101 packed column (6 ft × $^1/_8$ in.) and TCD detection, using helium as the carrier gas. Reaction products were identified by comparing the retention times of the known standard compounds. Unknown compounds were identified by gas chromatography−mass spectrometry using a 4500 Finnigan quadrupole mass spectrometer coupled with a Varian 3400 GC. A DB-1 capillary column (30 m × 0.25 mm) was used to separate the products.

Analyses of the Catalysts. The catalysts were characterized before and after the reactions. For this purpose, Auger electron spectroscopy (AES), atomic absorption spectroscopy (AA), scanning electron microscopy (SEM), and energy-dispersive X-ray spectroscopy

(EDX) were used. Some characterizations were also carried out after the catalysts were heated at 400 °C in the absence of reactants in either hydrogen or helium.

A PHI Model 545 AES was used to estimate the surface S/Fe ratio and the surface O/Fe ratio. The catalyst particles to be analyzed were first washed with methanol, to remove elemental sulfur formed during the disproportionation reaction, as described in Dadyburjor *et al.* (1994). Methanol dissolves both α and β forms of sulfur (Weast, 1979). The catalyst particles suspended in methanol were then dropped on an indium foil. The foil was dried in air and then transferred to the AES chamber. Care was taken simply to place the catalyst particles on the foil without using any mechanical force to press them into the foil. This approach was motivated by studies which showed that use of any mechanical force resulted in destruction of the catalyst surface. Species surface concentrations, determined by AES, are accurate to ±5 atomic % based on typical uncertainties in AES sensitivity factors.

SEM and EDX were used to study the morphology (size and shape) and the bulk chemical composition (S/Fe ratio) of the catalyst particles, respectively. A Hitachi SEM/EDX Model S-570 was used. Both SEM and EDX were simultaneously carried out on a catalyst sample. The initial preparation of the sample was the same as that used for AES analysis, except that the catalyst/methanol mixture was placed on a carbon sample stub and dried. The sample was then coated with carbon and transferred to the SEM/EDX for analysis. Species bulk concentration and concentration ratios, determined by EDX, are accurate to ±10 atomic % based on variation in atomic radii of elements (matrix effect) and particle size distribution variations.

AA is used to identify Fe in PH and PY in the iron sulfide catalysts. A Perkin-Elmer Model 2380 unit was used to find the amount of Fe in each of the sulfides. The procedure used was as follows. Approximately 0.05 g of the catalyst was taken in a glass filter with 15 mL of 6 M HCl. After 3−4 h, the acid (with dissolved PH) was filtered. All the glassware and the catalyst residue were washed two or three times with distilled water, and the volume was made up to 100 mL. This acidic solution was stored in a glass bottle as liquid A for further analysis. The catalyst residue in the filter was again mixed with 15 mL of 8 M HNO_3. After 3−4 h, the acid (with the dissolved PY) was filtered. All the glassware was again washed two or three times with distilled water. The volume of solution collected was made up to 100 mL and stored in a glass bottle as liquid B. The two solutions were analyzed on AA for their iron content. Standard solutions of 1−300 ppm Fe were used to calibrate the AA. The molar ratio PH/PY is calculated by

$$\text{PH/PY (molar ratio)} = \text{(Fe[ppm] in liquid A)/(Fe[ppm] in liquid B)} \quad (3)$$

The validity of this technique has been proven by AES analysis of the undissolved catalyst (Chadha, 1995), in that the characteristic lines for monoclinic pyrrhotite (Fe_7S_8) disappear after dissolution in HCl, while the lines for FeS_2 remain.

Results and Discussion

Activity of Iron-Sulfide-Based Catalysts in Model Reactions. (a) Hydrogenation. As noted earlier, phenanthrene hydrogenation from H_2(g) was studied at 400 °C and 1000 psig (cold) H_2. As a base line, the reaction was first performed in the absence of any catalyst. Then each of the five catalysts were used in turn. The results are reported as conversion, which is defined as

$$X_H\,(\%) = 100 \times \text{(products formed, mol)/(reactant added, mol)} \quad (4)$$

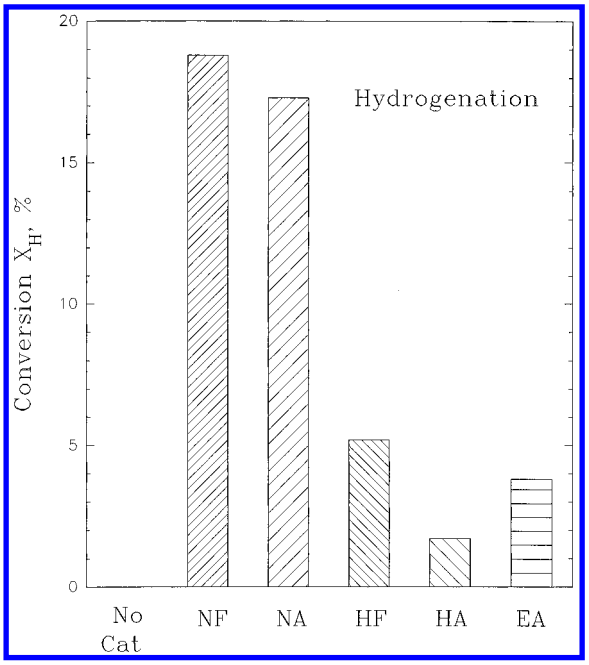

Figure 3. Results of the hydrogenation reaction under DCL conditions, using the five catalysts as described in the text.

No products were formed in the absence of the catalysts. This indicates that homogeneous reactions and reactor surface effects could be neglected. After the catalytic reactions, both 9,10-dihydrophenanthrene (DHPH) and 1,2,3,4-tetrahydrophenanthrene (THPH) were found in the products, as expected (Whitehurst *et al.*, 1980). However, due to difficulties with separation, both the isomers were combined in the determination of the moles of product. Octahydrophenanthrene (OHPH) and perhydrophenanthrene (PHPH) were not detected in the products.

Conversions from the hydrogenation experiments are shown in Figure 3. Negligible hydrogenation of phenanthrene is seen in the absence of a catalyst. The activity of the aged catalyst disproportionated in hydrogen, HA, though not negligible, is very low, corresponding to less than 2% activity under the experimental conditions. Under the same reaction conditions, the aerosol catalyst, EA, shows somewhat greater activity, almost 4% conversion. The freshly synthesized catalyst disproportionated in hydrogen, HF, gives an even higher conversion. The catalysts disproportionated in nitrogen report the highest activities by far, with the conversion using the fresh catalyst, NF, being slightly greater than that with the aged catalyst, NA.

Suzuki *et al.* (1989) studied the hydrogenation of phenanthrene, using 13 different iron- and molybdenum-based catalysts at 375 °C and 725 psig (cold) H_2. A 14.4% conversion of phenanthrene was observed using natural pyrite. Higher conversions (>25%) were seen when molybdenum-based catalysts were used. The present results fall in between these two extremes. While a quantitative comparison between these results

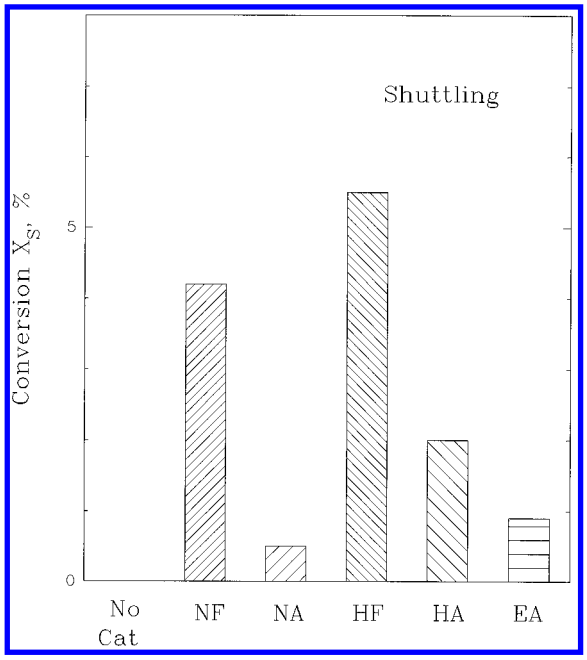

Figure 4. Results of the shuttling reaction under DCL conditions, using the five catalysts as described in the text.

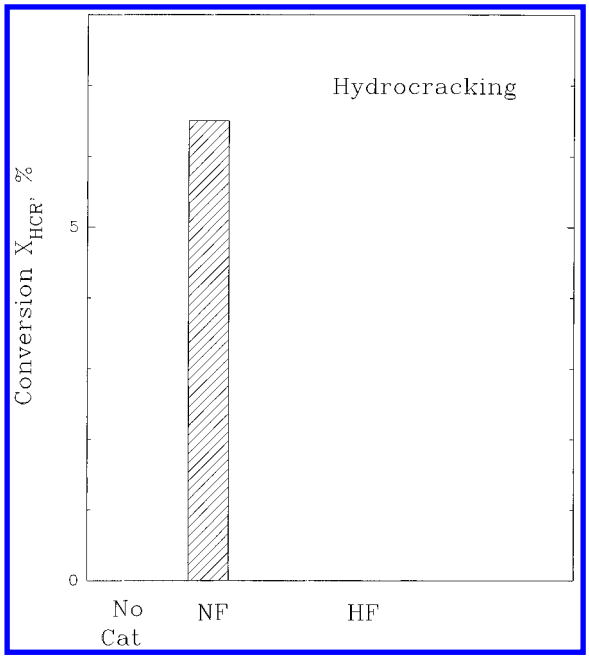

Figure 5. Results of the hydrocracking reaction under DCL conditions, using the five catalysts as described in the text.

and ours cannot be made because of the differences in catalyst types and reaction conditions, all the results indicate that iron-based catalysts have some capability for hydrogenation.

Analysis of the gas phase (on a hydrogen-free basis) after reactions with the fresh catalysts showed that H_2S was by far the major component, over 80%. These results are compared with those from other model reactions toward the end of this section.

(b) Shuttling Model Run. As noted earlier, the activity of the catalysts for hydrogen shuttling in the liquid phase was studied using phenanthrene hydrogenation from tetralin at 400 °C and 1000 psig (cold) He. From Figure 2, DHPH and THPH are the predicted reaction products. As before, the reaction was carried out first in the absence of a catalyst. Results are presented in Figure 4, using a percent conversion X_S analogous to that defined for hydrogenation by eq 4.

As for the vapor-phase hydrogenation reaction, no products can be detected in the absence of any catalyst. For the shuttling reaction, the highest activity is registered by the HF catalyst (5.5%), and significant activity is lost when the corresponding aged catalyst, HA, is used. The conversion obtained with the NF catalyst is almost as high as that with the HF catalyst. However, when the corresponding aged catalyst (NA) is used, the conversion is almost negligible (<0.5%). The conversion is similarly very small with the EA catalyst.

The fractions of H_2S formed in the gas phase during the shuttling reactions over the fresh catalysts are significant but smaller than those formed during hydrogenation. These results are discussed later.

(c) Cracking Model Run. As noted above, the cracking functionality of the catalysts (in the absence of hydrogen) was studied using cumene under conditions similar to the previous model reactions. The expected cracking reaction products are benzene and propylene (eq 1). In all the experiments, with or without the catalyst, benzene was not formed. Hence, the conversion corresponding to all the catalysts can be set equal to zero. Further, no H_2S was observed in the gas phase after any cracking reactions.

However, some other peaks were observed in the GC traces of the products. These were identified as benzothiophene (C_9H_8S) and benzo(*b*)thiophene (C_8H_6S) by GC−MS analysis. The quantity of these compounds in the products is very small (0.5%). The presence of these compounds is possible because of the reaction of sulfur (from the catalyst surface) with cumene. A similar interaction of the catalyst surface with model compounds was observed by Ogawa *et al.* (1984) in their analysis of the catalyst surface using Mössbauer spectroscopy.

(d) Hydrocracking Model Run. As noted earlier, the hydrocracking functionality was studied using diphenylmethane (DPM). Because of the unavailability of the aged catalysts, these reactions were carried out using only the fresh HF and NF catalysts. The results of Figure 5 indicate that significant hydrocracking is observed with the HF catalyst, whereas hydrocracking is negligible in the absence of a catalyst, or with the NF catalyst.

(e) Hydrogen Sulfide in Reaction Products. The percent H_2S in the gas phase produced is shown in Figure 6 for both fresh catalysts. Since hydrogen is used as a carrier gas in the GC, the H_2S content is obtained on a H_2-free basis. Figure 6 indicates that no H_2S is formed after cracking or after heating in He. Further, for both types of catalysts, the amount of H_2S produced in the shuttling model run is lower than those in the other runs. Presumably, while the presence of the hydrogen in the vapor phase during the other three processes facilitates a reaction of the sort

$$FeS_2 + (2 - x)H_2 \rightarrow FeS_x + (2 - x)H_2S \qquad (5)$$

the hydrogen contributed by the tetralin during the shuttling reaction does not form as much H_2S in the gas phase. The amount of H_2S produced in all the model runs with the HF catalyst is lower than that produced in runs with the NF catalyst. We return to this observation later.

(f) Summary of Activity Behavior. No cracking activity is seen for any catalyst. Hydrogenation activity is greatest in the NF catalyst, while the HF catalyst is

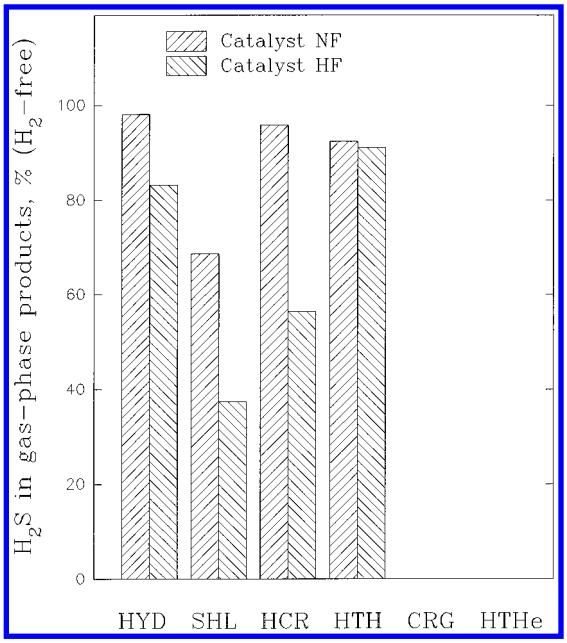

Figure 6. Fraction of hydrogen sulfide (on a hydrogen-free basis) in gas-phase products of model reactions over fresh catalysts NF and HF: HYD, hydrogenation; SHL, shuttling; HCR, hydrocracking; HTH, heating in hydrogen; CRG, cracking; HTHe, heating in helium.

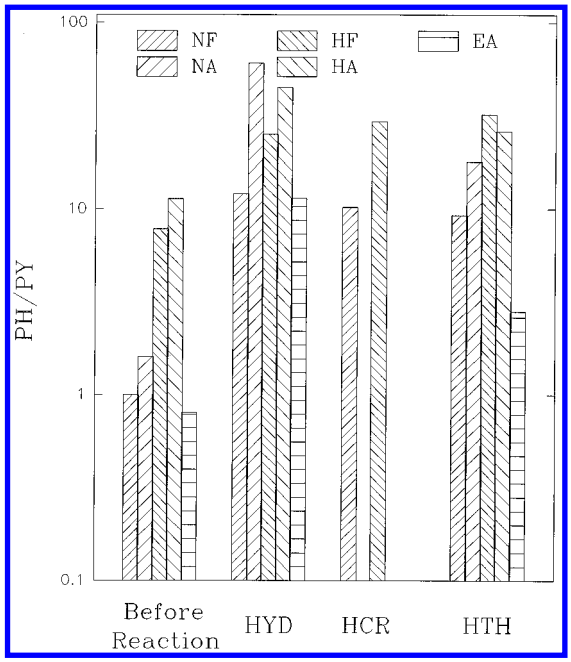

Figure 7. Ratio PH/PY for the five catalysts before reaction and after model reactions involving hydrogen in the gas phase. The reaction abbreviations are as in Figure 6.

superior for shuttling and hydrocracking. For both catalysts, aging leads to a slight loss of hydrogenation activity but a considerable loss of shuttling activity. The aged aerosol catalyst EA exhibits activity intermediate between those of the other two aged catalysts, HA and NA. In general, the gas-phase products contain a higher proportion of H_2S (on a hydrogen-free basis) for the NF catalyst and a smaller proportion of H_2S for the shuttling reaction.

Catalyst Characterization. (a) PH/PY Ratio. Figures 7 and 8 show the ratio of PH to PY in the catalysts before reaction and after reaction. Figure 7 deals with the processes involving vapor-phase hydrogen, *i.e.*, hydrogenation and hydrocracking reactions,

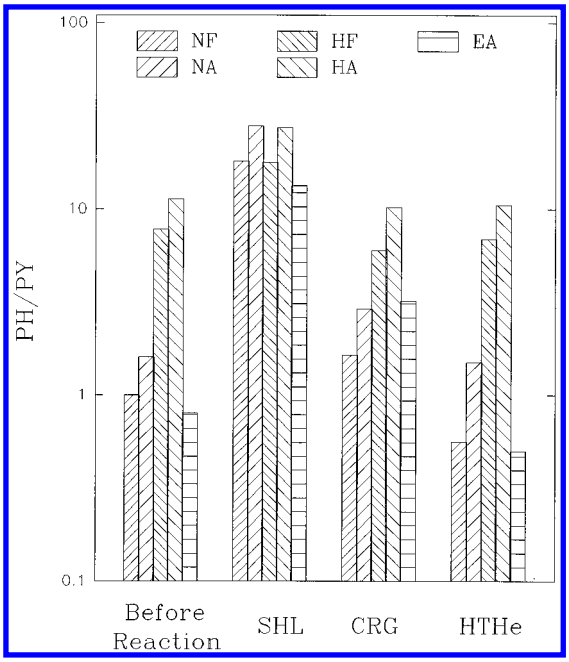

Figure 8. Ratio PH/PY for the five catalysts before reaction and after model reactions that do not involve hydrogen in the gas phase. The reaction abbreviations are as in Figure 6.

and heating in hydrogen. Figure 8 deals with the reactions not involving vapor-phase hydrogen, *i.e.*, shuttling and cracking, as well as the results when the catalysts are heated in He.

Catalyst NF has equal amounts of PH and PY before reaction. The work of Stansberry *et al.* (1993) indicated that this is a superior catalyst overall for coal liquefaction. Catalyst HF has an appreciably higher value of the ratio PH/PY. This is consistent with the H_2S data shown in Figure 6, in that the higher PY content of the NF catalyst reacts with hydrogen to produce a higher percentage of H_2S in the gas phase. When catalysts NF and HF are aged before reaction (to NA and HA, respectively), the PH/PY ratio increases to a small extent, approximately 50% greater than the fresh value. For catalyst EA, the PH/PY ratio is slightly less than unity, *i.e.*, approximately that of NF.

From Figure 7, it can be seen that the PH/PY ratios for all the catalysts increase markedly after reactions involving hydrogen in the gas phase. The increase is greatest for catalyst NA but is at least a factor of 3 for all of the catalysts. Again, the vapor-phase hydrogen can be expected to play a role, *via* eq 5. From Figure 8, shuttling causes an increase in the PH/PY ratio, but the change is generally small for all the other cases. It should be noted that shuttling involves hydrogen, though not in the vapor phase. For catalyst NF heated in He, the value of PH/PY decreases appreciably. Under these experimental conditions, catalyst "reconstruction" is possible (Lee and Montano, 1984). The elemental sulfur formed during the catalyst disproportionation (eq 1) could react with the PH to form a pyrrhotite richer in sulfur:

$$FeS_{x_1} + (x_2 - x_1)S \rightarrow FeS_{x_2} \qquad (6)$$

or even PY ($x_2 = 2$).

Similar observations have been made by Ogawa *et al.* (1984), Hei *et al.* (1986). Montano *et al.* (1986), Baldwin and Vincinguerra (1983), and Thomas *et al.* (1982). Huffman *et al.* (1993) have seen (from Mössbauer and EXAFS spectroscopic analysis of the catalysts) that the

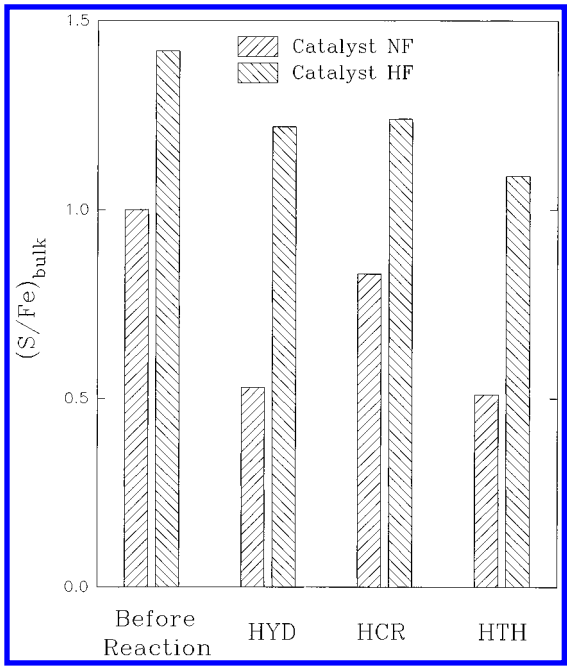

Figure 9. Ratio (S/Fe) in the bulk for fresh catalysts NF and HF before reaction and after model reactions involving hydrogen in the gas phase. The reaction abbreviations are as in Figure 6.

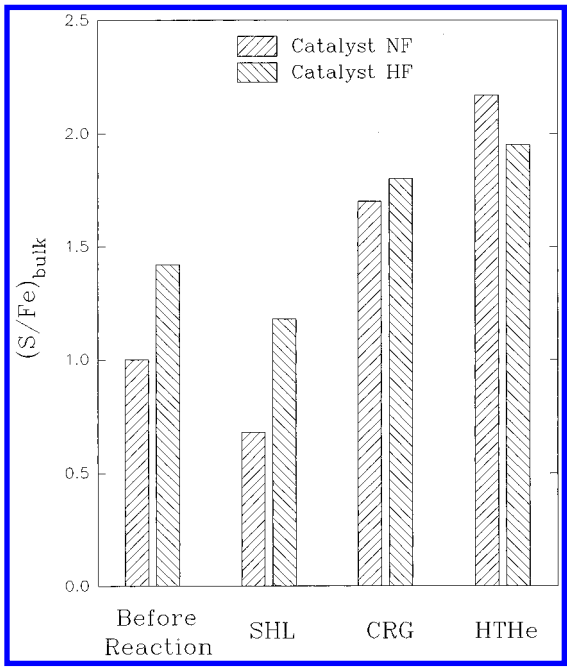

Figure 10. Ratio (S/Fe) in the bulk for fresh catalysts NF and HF before reaction and after model reactions that do not involve hydrogen in the gas phase. The reaction abbreviations are as in Figure 6.

catalysts obtained after DCL in a hydrogen atmosphere are highly pyrrhotitic in nature.

(b) Bulk Analysis—S/Fe. The sulfur-to-iron ratios, $(S/Fe)_{bulk}$, in the bulk of the catalysts NF and HF were obtained by EDX analyses. Recall that the catalysts were washed in methanol prior to the EDX measurements, so that the elemental S (or at least that on the external surface) was removed. Values of $(S/Fe)_{bulk}$ for the catalysts before reaction, reacted in a hydrogen atmosphere and in helium, are shown in Figures 9 and 10. Before reaction, $(S/Fe)_{bulk}$ for HF is very close to the stoichiometric value of 1.5 for Fe_2S_3. Further, no iron was found to dissolve into the methanol solvent. Hence, for catalyst HF, it is reasonable to assume that little elemental S was present (on the surface, at least) to be removed by washing, $(S/Fe)_{bulk}$ for NF is lower than 1.5, presumably because elemental S on the surface was removed by washing prior to EDX.

From Figure 9, the value of $(S/Fe)_{bulk}$ decreases after reaction with hydrogen. This is expected, since (elemental and bonded) sulfur from the catalyst bulk reacts with $H_2(g)$ to form $H_2S(g)$, whereby the sulfur contents of the catalysts decrease. The decrease is greater for NF than for HF and for heating in hydrogen than for the two model reactions. From Figure 10, the value of $(S/Fe)_{bulk}$ decreases after the shuttling run, consistent with the role of the hydrogen-donating solvent in the other measurements above. In the absence of $H_2(g)$ or a H-donor, however, the bulk S/Fe ratio increases after reaction. This indicates the possibility of further reaction (as in eq 6) of the PH with elemental S to form a PH richer in S, or even PY. (Note that the methanol wash to remove the elemental S occurred always after the reaction, before the analysis.) The increase in $(S/Fe)_{bulk}$ is consistent with the decrease in the PH/PY ratio seen in Figure 8 after heating in He.

(c) Surface Analysis—S/Fe. Surface changes in the sulfur-to-iron ratio, $(S/Fe)_{sfce}$, have been studied by AES. The analyses were performed on the catalyst samples obtained after the duplicate model runs. Repetitive analyses were also performed on the freshly synthesized catalysts. The results are shown in Tables 1 and 2 for catalysts NF and HF, respectively. The value of $(S/Fe)_{sfce}$ for NF before any reaction is 1.2, whereas the corresponding value for HF varies but is centered around 1.9. Note that the elemental S on the surface of both NF and HF was removed before the AES analysis was carried out. It is reasonable to expect that, during the preparation of the HF catalyst, disproportionation in hydrogen removes most of the surface elemental S, while it is still left for the NF catalyst, to be removed by pretreatment prior to AES. The surface of the HF catalyst appears to contain less PH than does that of NF, or at least the PH is richer in S for HF than for NF. Interestingly, as noted above, the (bulk) PH/PY ratio is larger for HF than for NF.

After the model runs in general, a wide range of values of $(S/Fe)_{sfce}$ are observed. For one hydrogenation run (using NF as the catalyst, Table 1), the ratio varies from 0.9 to 2.3, whereas for another, it varies from 0.2 to 1.4. A statistical test of the data points for this case shows a value of the "t-test parameter", t, equal to 2.76, corresponding to less than 95% probability, apparently not a high probability, that the two runs are statistically different. (For t-tests, a 99% probability is considered as a reasonable confidence level for the two runs not to be significantly different [Harris, 1987].) Similarly, the variations in the surface ratio for the other model runs are observed to be large but perhaps not statistically significant. As a rule, the values of t appear to be lower when hydrogen is not involved in the catalyst manufacture or the process. The surface uniformity of the NF catalyst disappears after any model run.

Poor reproducibility of the surface ratios is possibly because of nonuniformity of the catalyst surface. It is also possibly due to the small number of data points taken for each catalyst sample to find the $(S/Fe)_{sfce}$ ratio. In general, five spots are taken on a catalyst sample, and line averages at each of these five spots are calculated. Unfortunately, there are practical limitations to taking more data points. Using more than five spots results in sample charging, where the substrate

Table 1. Surface Ratios (S/Fe) from AES Analysis of Catalyst NF

	$(S/Fe)_{sfce}$					
reaction	range	mean	std. dev.	variance	value of *t*	probability of significant difference
before	1.09−1.29	1.19	0.08	0.008		0
	1.19−1.29	1.19	0.1	0.01		
hydrogenation	0.9−2.3	1.73	0.52	0.27	2.76	95
	0.2−1.4	0.88	0.45	0.2		
shuttling	0.5−1.8	1.11	0.17	0.03	2.47	95
	0.5−1.9	0.82	0.2	0.04		
cracking	0.6−2.2	1.36	0.63	0.40	0.759	50
	0.9−2.3	1.67	0.66	0.43		
hydrocracking	0.4−2.8	0.65	0.87	0.75	1.722	85
	0.2−2.2	1.7	1.05	1.12		
heat in H_2	0.6−2.6	1.54	0.81	0.65	0.94	60
	0.7−3.0	2.04	0.87	0.76		
heat in He	1.9−4.0	2.73	0.82	0.67	0.42	30
	1.7−3.3	2.54	0.59	0.34		

Table 2. Surface Ratios (S/Fe) from AES Analysis of Catalyst HF

	$(S/Fe)_{sfce}$					
reaction	range	mean	std. dev.	variance	value of *t*	probability of significant difference
before	1.3−4	1.92	1.17	1.37		0
	1.2−3.5	1.91	1.17	1.37		
hydrogenation	0.89−2.3	1.81	0.84	0.71		0
	1.2−3.8	1.82	1.11	1.24		
shuttling	1.2−2.6	1.52	0.61	0.38	0.927	60
	1.6−2.5	1.82	0.39	0.15		
cracking	1.5−1.8	1.59	0.12	0.01	4.919	95
	1.2−1.4	1.26	0.09	0.01		
hydrocracking	1.2−3.5	1.72	1.0	1.0	1.834	85
	1.1−4	2.12	1.21	1.49		
heat in H_2	0.4−1.7	1.54	0.81	0.65	3.069	95
	1.9−3.4	2.04	0.87	0.76		
heat in He	3.0−4.6	2.73	0.82	0.67	4.685	95
	1.9−2.2	2.54	0.59	0.34		

Table 3. Surface Ratios (O/Fe) from AES Analysis of Catalysts

catalyst type	$(O/Fe)_{sfce}$	catalyst type	$(O/Fe)_{sfce}$
NF	2.28	HF	0.81
NA	2.9	HA	1.55

captures electrons or ions and becomes negatively charged. The charge-up continues until the surface potential reaches the value of that of the incident electron beam (Chang, 1974). For this reason, it was not possible to take more data points, even though that might have improved the statistical significance of the surface analysis.

Because of the variability of the $(S/Fe)_{sfce}$ values, it is not possible to state unequivocally that these values increase or decrease after the model runs. In most cases, the average of the values appears relatively unchanged. The one exception appears to be heating in He. In this case, the value of the ratio increases, for both NF and HF, to a value of 2.6. The increase in the value of the surface ratio is consistent with the increase in the value of the bulk ratio noted earlier.

(d) Surface Analysis—O/Fe. Since no special precautions were taken to isolate the catalysts from air, an oxygen signal was obtained during all AES runs. The concentration of oxygen on the catalyst surface is reported in Table 3 for catalysts NF, NA, HF, and HA before the model reactions. The catalytic surface before reaction is much more uniform in terms of the oxygen distribution than it is with respect to the S; hence, only the average values are presented. Oxygen concentrations after the model runs showed no consistent variation in value and are not reported.

The $(O/Fe)_{sfce}$ ratio for catalyst NF is significantly larger than that for catalyst HF. Since the NF catalyst is more active for direct coal liquefaction than is catalyst HF (Stansberry *et al.*, 1993), it would appear that the oxygen adsorbs more on the more-active catalyst. From Table 3, the aged catalysts typically have larger values of $(O/Fe)_{sfce}$ than those for the corresponding fresh catalyst. Clearly, our aging process results in an increased adsorption of oxygen on the surface. The increase is proportionately small for the NA catalyst (relative to the NF catalyst) but is significant for the HF catalyst; even so, after aging, the ratio $(O/Fe)_{sfce}$ is greater for NA than for HA. The more-active catalyst would appear to have more sites available on which the oxygen could adsorb.

(e) Morphological Changes. SEM was used to characterize the morphology of the catalyst particles, before and after each model run. The results are less quantitative than those described above but may help in obtaining an overall view of the model runs.

Figure 11 shows a SEM of catalyst NF. The particle size is approximately 1 μm. The particles do not have a definite shape. A low degree of agglomeration is seen, limited to 2−3 particles. Figure 12 shows a SEM of the catalyst HF. The catalyst particles are seen to form an agglomerated mass of micron-sized particles.

During the preparation of catalyst NF, the precursor Fe_2S_3 is heated (disproportionated) in nitrogen at 200 °C for 1 h without any agitation. This material does not agglomerate (Figure 11). However, when the same precursor is treated with hydrogen at 375 °C for 1 h (without any agitation), to form the hydrogen-disproportionated catalyst HF, agglomeration is observed (Figure 12). It seems that the particles tend to agglomerate somewhere in the temperature range of 200−400 °C. Under reaction (liquefaction) conditions, the exposure of the catalyst particles to a high temperature (400 °C) for 30 min and the agitation of the catalyst can

Figure 11. Scanning electron micrograph of catalyst NF before reaction.

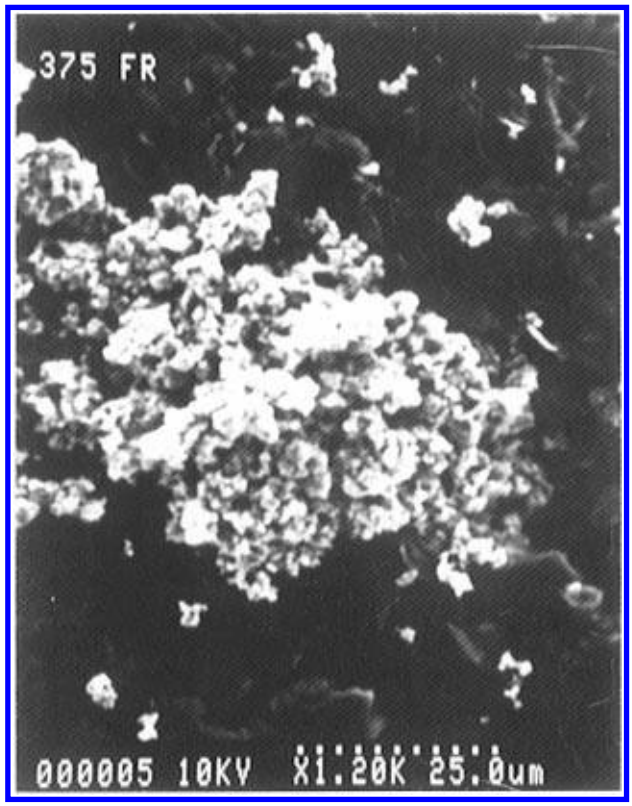

Figure 12. Scanning electron micrograph of catalyst HF before reaction.

be expected to bring these particles close enough to agglomerate and to transform as shown here.

Figure 13 is a SEM of an agglomerate of particles obtained after heating catalyst NF in He at 400 °C. The particles seen here are transformed to form flat surfaces. The size of the agglomerate is approximately 50 μm. Figure 14 is a SEM of NF after the shuttling model run. It is interesting to note the high degree of agglomeration

Figure 13. Scanning electron micrograph of catalyst NF after heating in He(g). The micrograph shows transformation of the catalyst particles to agglomerates of size 50−60 μm.

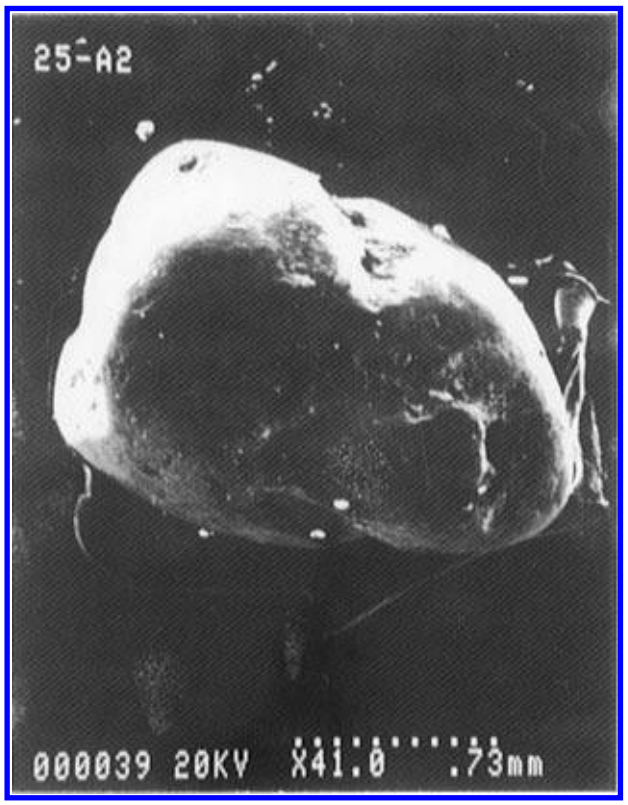

Figure 14. Scanning electron micrograph of catalyst NF after shuttling reaction.

here: the particles agglomerate from micron size to form large particles of size 1−2 mm. Distinct cavities can be seen on the surface of the agglomerates. This gives a porous appearance to the agglomerated mass. Figure 15 is a high-magnification micrograph of the agglomerated catalyst showing individual catalyst particles.

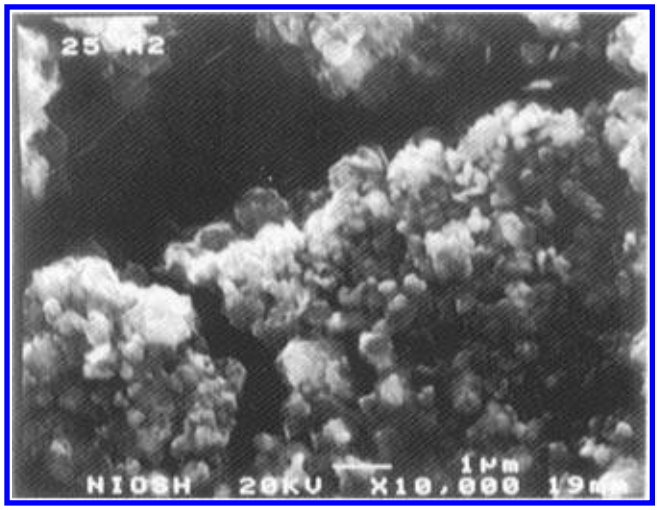

Figure 15. Scanning electron micrograph of catalyst NF after shuttling reaction. The micrograph shows a high-magnification picture of the agglomerate shown in Figure 14. The agglomerated particles are seen clearly in this micrograph.

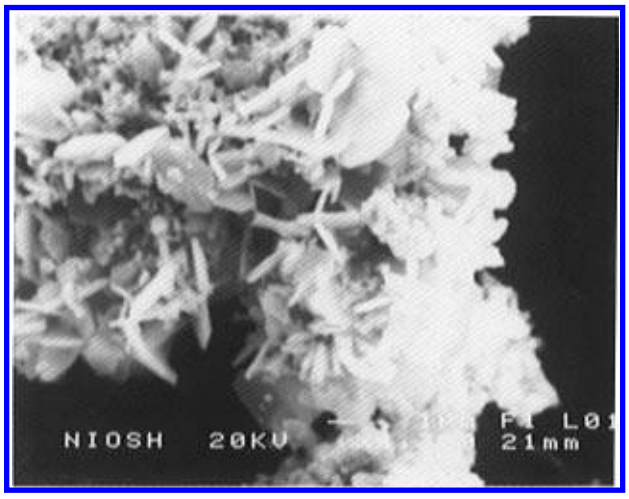

Figure 16. Scanning electron micrograph of catalyst HF after hydrocracking model run. The micrograph shows the needle-shape catalyst formed.

Agglomeration of the catalyst particles is seen after all the model reactions. In most cases, the agglomerated particles are similar to those seen in Figures 14 and 15. However, for catalyst HF after the hydrocracking model run, a slightly different behavior is seen, as shown in Figure 16. Agglomeration is seen, as before. However, needlelike structures, or possibly platelets, are also observed in the micrograph. These structures were not observed after other runs with the HF catalyst or with other hydrocracking reactions.

(f) Summary of Catalyst Characterization. As prepared, the NF catalyst contains roughly equal amounts of PH and PY in the bulk. The ratio PH/PY is significantly greater for the HF catalyst. Aging increases the PH/PY ratio to some extent for all catalysts. The surface of HF is less uniform than that of NF, as evidenced by the wider range of values of the surface ratios $(S/Fe)_{sfce}$ for the former. On an elemental-S-free basis, the value of $(S/Fe)_{sfce}$ is greater for HF than for NF. Hence, the HF surface contains less PH than does the NF surface, even though the PH/PY ratios indicate that the situation is reversed for the bulk. The bulk ratio $(S/Fe)_{bulk}$ for HF is approximately the stoichiometric value of 1.5 and is greater than that for NF. This implies that NF contains elemental S, at least on the surface (to be washed away during the methanol pretreatment), whereas HF contains relatively little elemental S, at least on the surface. The slightly higher temperatures used for the synthesis of HF result in some agglomeration relative to NF.

During the model reactions, the agglomeration is more severe. Also, the ratio PH/PY changes. It increases in the presence of hydrogen, more so when the hydrogen is in the vapor phase, presumably due to the conversion of PY to PH and the loss of H_2S. Concurrently, $(S/Fe)_{bulk}$ decreases. The surface ratio $(S/Fe)_{sfce}$ is still spread out over a wide range and does not appear to change noticeably. After heating in He, the PH/PY ratios decrease for all catalysts tested, and $(S/Fe)_{bulk}$ values increase for both NF and HF, presumably due to surface and bulk reconstruction when PH recombines with elemental S to form PY. Under the same conditions, the surface ratio $(S/Fe)_{sfce}$ can also be seen to increase, at least for the NF catalyst.

Effect of Key Parameters on Catalyst Activity. The variation in the activity of the catalysts used in this work can be discussed with reference to three factors: the nature of the bulk catalyst (as quantified by the ratios PH/PY and $(S/Fe)_{bulk}$), the nature of the catalyst surface (as quantified by the ratios $(S/Fe)_{sfce}$ and $(O/Fe)_{sfce}$), and the catalyst age.

(a) Bulk Catalyst Properties. The catalyst NF, which possesses the highest activity for hydrogenation, contains roughly equal amounts of PH and PY. For HF, on the other hand, approximately 90% of the Fe is present as PH. This catalyst possesses the highest activity for shuttling and hydrocracking. Hence, it would appear that the PY present initially in the catalyst seems to play an active role in hydrogenation, whereas PH appears to be important for the shuttling and hydrocracking activity of a catalyst.

Significantly, no catalyst tested in this work showed any activity for cracking, yet these catalysts are significantly active in direct coal liquefaction (DCL). Hence, hydrocracking, rather than cracking, would appear to be important in DCL.

During the model reactions, the presence of hydrogen (in the vapor phase or contributed by the solvent) increases the PH content at the expense of the PY, following eq 5. This should decrease hydrogenation and improve shuttling and hydrocracking. However, the catalyst particles tend to agglomerate, and this can be expected to reduce the activity for all reactions. For DCL, we have found that the most active form of the catalyst is that prepared by *in-situ* impregnation into the coal (Liu *et al.*, 1996; Chadha *et al.*, 1996). It is reasonable to expect that this technique minimizes the agglomeration during the reaction process.

In the absence of hydrogen, the high temperatures cause PY to be formed at the expense of PH and S, following a surface reconstruction (eq 6).

(b) Surface Catalyst Properties. The NF catalyst, which has the highest hydrogenation activity, appears to have a large amount of elemental S present, on the external surface at least. Perhaps the sulfur helps to stabilize the catalyst against decomposition during hydrogenation and DCL conditions. This is consistent with the hypothesis of Thomas *et al.* (1982). The NF catalyst, when exposed to air, also contains a significant amount of oxygen on the surface. Perhaps the oxygen is adsorbed on potential active sites for hydrogenation.

The HF catalyst, active in shuttling and hydrocracking, is characterized by an extremely nonuniform surface. The uniformity reduces even further when the

catalyst is heated in hydrogen. Heating in He reconstructs the surface, as noted above. The variability on the catalyst surface could be a result of catalyst agglomeration or H_2S interaction with the catalyst. It is difficult to relate the activity of the catalysts to the catalyst surface properties, solely on the basis of this observation. However, varying $(S/Fe)_{sfce}$ ratios on the catalyst surface indicate the possible presence of S-rich and S-deficient sites on the catalyst surface, as indicated by Ogawa *et al.* (1984) in their study of DPM hydrocracking. The Fe-vacant sites on the catalyst surface were believed to weaken the H−SH bond of H_2S, forming H atoms.

(c) Catalyst Age. For catalyst NA compared with NF, the hydrogenation activity decreases marginally. However, a large drop is seen in the shuttling activity. For the HA catalyst, the hydrogenation activity and the shuttling activity are both decreased to about the same extent, relative to the HF catalyst. The effect of age on activity is not mirrored well by the PH/PY ratio or by the ratio $(O/Fe)_{sfce}$. The catalyst hydrothermally disproportionated in nitrogen seems to be a more stable hydrogenation catalyst, but it is not a stable shuttling catalyst. The catalyst disproportionated in hydrogen is neither a stable hydrogenation catalyst nor a stable shuttling catalyst.

A Preliminary Physical Model. Based on the surface, bulk, and morphological changes in the catalyst, a preliminary physical model is proposed for an iron-sulfide-based catalyst in different reacting atmospheres. Initially, the 1−2 μm size catalyst particles are intimate mixtures of FeS_x and FeS_2 (PH and PY). These also have a uniform catalyst surface with Fe and S sites. Once these particles undergo model reactions in H_2 or He atmospheres, the bulk and surface of the catalyst undergo different changes. A pictorial representation of the changes is shown in Figure 17.

In the presence of hydrogen, the main reaction in the bulk is the conversion of PY to PH, following eq 5. This increases the PH/PY ratio, as observed. The H_2S formed in this reaction diffuses to the surface, where some reacts locally to form PY (by the reverse of eq 5) or a PH richer in S, *via*

$$FeS_{x_1} + (x_2 - x_1)H_2S \rightarrow FeS_{x_2} + (x_2 - x_1)H_2 \quad (7)$$

Equation 5 can also take place locally on the surface. The combination of eq 5, its reverse, and eq 7 results in highly variable local ratios of S/Fe on the catalyst surface, with some regions being S-rich while others are S-poor. The S-rich areas of Figure 17A are indicated by shading, with the solid areas indicating elemental S (formed during the catalyst disproportionation).

In the presence of He, there is no interconversion of PY and PH. However, it is possible that the elemental sulfur reacts with the PH on the surface of the catalyst to form PH with a larger value of x, as in eq 6. This would lead to the larger value of the ratio $(S/Fe)_{sfce}$ observed after washing with methanol. In any case, the surface is more uniform, as is shown by the lighter shading in Figure 17B.

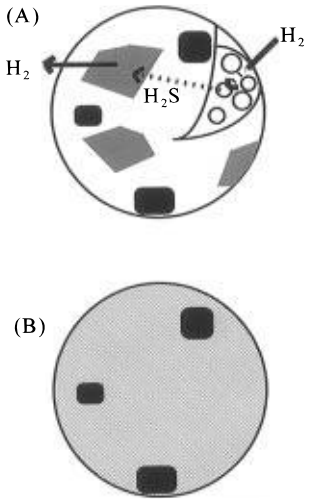

Figure 17. Pictorial representation of changes in catalyst: (A) in the presence of hydrogen; (B) in the absence of hydrogen (He atmosphere). In A, the broken and whole arrows denote transfer within and outside the catalyst, respectively, the gray patches denote regions richer in sulfur, the white areas are S-deficient, and the small circles in the cutaway denote PY which is converted to PH. Dark patches in A and B denote elemental S. In B, the shading indicates that the catalyst surface is more uniform than in A.

Summary and Conclusions

1. A scheme of model DCL reactions was developed to study the hydrogenation, shuttling, hydrocracking, and cracking activity of five ferric-sulfide-based catalysts at DCL conditions. The catalyst precursor ferric sulfide disproportionates into PH, PY, and elemental S. These model DCL reactions offer a simple, reproducible, and quick means to study the different functionalities of the components of the catalysts.

2. The performance of the catalysts was seen to vary with the initial PH/PY ratio and age. Freshly prepared catalyst hydrothermally disproportionated in nitrogen (with PH/PY $\approx$ 1) was found to have the highest hydrogenation and hydrocracking activity, whereas the freshly prepared catalyst hydrothermally disproportionated in hydrogen (PH/PY $\approx$ 8) was found to be an active shuttler. In all the cases, the cracking activity was negligible. Aging was seen to have an adverse effect on catalyst activity. A larger drop was seen in the shuttling activity than in the hydrogen activity. The aged aerosol catalyst exhibited hydrogenation and shuttling activities intermediate between the two other aged catalysts.

3. Among the constituents of the ferrice-sulfide-based catalysts, PY seems to be important for catalyst hydrogenation activity, whereas PH seems to contribute to the shuttling activity of the catalyst.

4. The catalysts were characterized by AES, SEM, EDX, and AA to study the changes in surface, bulk, and morphology of the catalyst. After reaction in a hydrogen atmosphere, the bulk PH/PY values increased. Not much change in these values was observed in a helium atmosphere. The surface uniformity of the catalyst decreased in the model reactions. This is because of catalyst surface interactions with H_2S. Agglomeration of catalyst particles was found to increase during the model reactions, due to the exposure of the catalyst to high temperatures (>375 °C) for long times (>30 min) under agitated conditions. For the hydrocracking model run, needle-shaped structures were found in the SEM.

5. A simplified preliminary model was developed to explain the changes in surface and bulk characteristics of the catalyst. The model incorporates the hydrogenation of PY to PH and H_2S. The further interaction of H_2S with the catalyst surface makes it nonuniform, with S-deficient and S-rich sites. In the absence of hydrogen, surface reconstruction involves elemental S (from the

disproportionation of the ferrice sulfide) interacting with PH to form PH with a larger value of x.

Acknowledgment

The authors thank Dr. Peter Stansberry and Dr. Ramesh Sharma for their help in experimentation and Jianli Yang for her help with atomic absorption spectroscopy. Joel Harrison (at the National Institute for Occupational Safety and Health) and Lorraine Probert (at the College of Mineral and Energy Resources) are acknowledged for their help with scanning electron microscopy, and John Sinsel is acknowledged for his assistance in the surface analyses of the catalysts. This work was conducted under U.S. Department of Energy Contract DE-FC22-93PC93053 under the Cooperative Agreement with the Consortium for Fossil Fuel Liquefaction Science.

Literature Cited

Baldwin, R.; Vincinguerra, S. Coal Liquefaction Catalysis: Iron Pyrite and Hydrogen Sulfides. *Fuel* **1983**, *62*, 498.

Chadha, A. Activity and Changes of Iron-Sulfide-Based Catalysts in Model Coal Liquefaction Reactions. MSChE Thesis, West Virginia University, Morgantown, WV, 1995.

Chadha, A.; Sharma, R. K.; Stinespring, C. D.; Dadyburjor, D. B. Iron Sulfide Catalysts for Coal Liquefaction Prepared Using a Micellar Technique. *Ind. Eng. Chem. Res.* **1996**, *35*, 2916.

Chang, C. C. *Analytical Auger Electron Spectroscopy*; Plenum: New York, 1974.

Dadyburjor, D. B.; Stewart, W. R.; Stiller, A. H.; Stinespring, C. D.; Wann, J.-P.; Zondlo, J. W. Disproportionated Ferric Sulfide Catalysts for Coal Liquefaction. *Energy Fuels* **1994**, *8*, 19.

Derbyshire, F. Role of Catalysis in Coal Liquefaction Research and Development. *Energy Fuels* **1989**, *3*, 273.

Farcasiu, M.; Smith, C. Modeling Coal Liquefaction. 1. Decomposition of 4-(1-naphthylmethyl)bibenzyl Catalyzed by Carbon Black. *Energy Fuels* **1991**, *5*, 83.

Guin, J. A.; Lee, J. M.; Fan, C. W.; Curtis, C. W.; Lloyd, J. L.; Tarrer, A. R. Pyrite-Catalyzed Hydrogenolysis of Benzothiophene at Coal Liquefaction Conditions. *Ind. Eng. Chem. Process Des. Dev.* **1980**, *19*, 440.

Harris, D. C. *Quantitative Chemical Analysis*, 2nd ed.; W. H. Freeman and Co.: New York, 1987.

Hei, R. D.; Sweeny, P. G.; Stenberg, V. I. Mechanism of the Hydrogen-Sulphide-Promoted Cleavage of the Coal Model Compounds: Diphenylether, Diphenylmethane and Bibenzyl. *Fuel* **1986**, *65*, 577.

Huffman, G. P.; Ganguly, B.; Zhao, J.; Rao, K. R. P. M.; Shah, N.; Feng, Z.; Huggins, F. E.; Taghiei, M. M.; Lu, F.; Wender, I.; Pradhan, V. R.; Tierney, J. W.; Seehra, M. S.; Ibrahim, M. M.; Shabtai, J.; Eyring, E. M. Structure and Dispersion of Iron-Based Catalysts for Direct Coal Liquefaction. *Energy Fuels* **1993**, *7*, 285.

Kamaya, Y.; Nagae, S.; Oikawa, S. Effect of Coal Minerals on the Thermal Treatment of Aromatic Ethers and Carbonyl Compounds. *Fuel* **1993**, *62*, 30.

Lee, Y. C.; Montano, P. A. An Auger and EELS Study of Iron Sulfide (FeS_2, Fe_7S_8 and FeS) Surfaces. *Surf. Sci.* **1984**, *143*, 442.

Liu, Z.; Dadyburjor, D. B. Activity, Selectivity, and Deactivation of High-Sodium HY Zeolite. *J. Catal.* **1992**, *134*, 583.

Liu, Z.; Yang, J.; Zondlo, J. W.; Stiller, A. H.; Dadyburjor, D. B. *In Situ* Impregnated Iron-Based Catalysts for Direct Coal Liquefaction. *Fuel* **1996**, *75*, 51.

Malhotra, R.; McMillen, D. F. Relevance of Cleavage of Strong Bonds in Coal Liquefaction. *Energy Fuels* **1993**, *7*, 227.

Montano, P. A.; Stenberg, V. I.; Sweeny, P. *In Situ* Study of the Hydrogention of Diphenyl Ether in the Presence of Pyrrhotite and H_2S. *J. Phys. Chem.* **1986**, *90*, 156−159.

Ogawa, T.; Stenberg, V. I.; Montano, P. A. Hydrocracking of Diphenylmethane: Roles of H_2S, Pyrrhotite and Pyrite. *Fuel* **1984**, *63*, 1660.

Stansberry, P. G.; Wann, J.-P.; Stewart, W. R.; Yang, J.; Zondlo, J. W.; Stiller, A. H.; Dadyburjor, D. B. Evaluation of a Novel Mixed Pyrite/Pyrrhotite Catalyst for Coal Liquefaction. *Fuel* **1993**, *72*, 793.

Stiller, A. H.; Dadyburjor, D. B.; Stinespring, C. D.; Chadha, A.; Tian, D.; Martin, S. B.; Agarwal, S. Preparation of Iron-Sulfide-Based Catalysts using an Aerosol Technique. *Prepr.—Am. Chem. Soc., Div. Pet. Chem.* **1995**, *40*, 44.

Suzuki, T.; Yamada, H.; Sears, P. L.; Watanabe, Y. Hydrogenation and Hydrogenolysis of Coal Model Compounds by using Finely Dispersed Catalysts. *Energy Fuels* **1989**, *3*, 707.

Sweeny, P. G.; Stenberg, V. I.; Hei, R. D.; Montano, P. A. Hydrocracking of Diphenylether and Diphenylmethane in the Presence of Iron Sulphides and Hydrogen Sulphide. *Fuel* **1987**, *66*, 532.

Thomas, M. G.; Padrick, T. D.; Stohl, F. V.; Stephens, H. P. Decomposition of Pyrite Under Coal Liquefaction Conditions: A Kinetic Study. *Fuel* **1982**, *61*, 761.

Vernon, L. W. Free Radical Chemistry of Coal Liquefaction: Role of Molecular Hydrogen. *Fuel* **1980**, *59*, 102.

Weast, R. C., Ed. *CRC Handbook of Chemistry and Physics*, 60th ed.; CRC Press: Boca Raton, FL, 1979.

Whitehurst, D. D.; Mitchell, T. O.; Farcasiu, M. *Coal Liquefaction: The Chemistry and Technology of Thermal Processes*; Academic Press: New York, 1980.

Received for review July 26, 1996
Revised manuscript received October 30, 1996
Accepted November 7, 1996[⊗]

IE960455Q

[⊗] Abstract published in *Advance ACS Abstracts*, December 15, 1996.